Polymer 51 (2010) 1341–1354

Contents lists available at ScienceDirect

Polymer

journal homepage: www.elsevier.com/locate/polymer

Localization of carbon nanotubes at the interface in blends of polyamide and ethylene–acrylate copolymer

Anne-Christine Baudouin, Jacques Devaux*[,1], Christian Bailly*

Unité de Chimie et de Physique des Hauts Polymères, Université catholique de Louvain, B-1348 Louvain-La-Neuve, Belgium

ARTICLE INFO

Article history:
Received 25 September 2009
Received in revised form
15 January 2010
Accepted 20 January 2010
Available online 2 February 2010

Keywords:
Carbon nanotubes
Polymer blends
Interfacial confinement

ABSTRACT

The present study demonstrates for the first time the possibility to jam unpurified and unfunctionalized multiwall carbon nanotubes (MWNTs) at the interface of an immiscible blend of polyamide (PA) and ethylene–acrylate (EA) copolymer. The confinement appears to be stable. The influence of the mixing strategy and of the polyamide type used has been examined. When the MWNTs are first dispersed in PA6, most of them migrate to the interface although some of them stay in the PA phase. When the MWNTs are first dispersed in PA12, they remain well dispersed in PA. When the MWNTs are first dispersed in the EA copolymer or when the three components are simultaneously mixed, a large part of the MWNTs migrate to the interface whatever the PA used. However, some of the MWNTs remain in the EA phase and when PA12 is used, part of the MWNTs penetrate inside the PA nodules. By a combination of TGA and separation techniques, we show that the first polymer to come in contact with the nanotubes during melt mixing is (at least partially) adsorbed irreversibly, by non-covalent adsorption. The resulting modification of interfacial thermodynamics explains the observed confinement.

1. Introduction

The use of polymer blends as composites matrices to produce conductive materials at low conductive filler content has been studied for more than two decades. In 1987, Geuskens et al. [1] studied the electrical conductivity of polymer blends containing carbon blacks. They showed that the conductivity of rubber/polyethylene blends filled with carbon black is much higher than the conductivity of the polymer filled with carbon black at the same loading level. Such a result was explained by the selective localization of the carbon black particles in the multiphase polymeric system. This concept is known as double percolation. The carbon black-filled blend phase percolates (first percolation) and the carbon black forms a network within the percolated blend phase (second percolation). More recent studies [2–5] have also exploited the concept of double percolation for different blend systems and different conductive fillers. Among them, carbon nanotubes have attracted tremendous attention since their discovery in 1991 by Sumio Iijima [6]. They present unique atomic structure and properties such as very high aspect ratio (1000–10,000), high strength to weight ratio, high mechanical properties, and high thermal and electrical conductivities [7–13]. The concept of double percolation using carbon nanotubes has been studied to improve the electrical conductivity of polymer blends. Pötschke et al. [14,15] have worked with composites of polycarbonate (PC) filled with multiwall carbon nanotubes (MWNTs). These composites were then mixed with polyethylene (PE) in order to get cocontinuous structures exhibiting double percolation. The MWNTs were found to stay in the PC phase. The authors have also studied blends of PC containing MWNTs with PP containing nanoclay [16]. The MWNTs stay well dispersed in the PC while the nanoclay migrates from PP towards the interface. Wu and Shaw [17,18] have studied composites of poly(ethylene terephtalate) (PET) filled with MWNTs. These formulations were then mixed with poly(vinylidene fluoride) (PVDF), polypropylene (PP), high density polyethylene (HDPE) or polyamide 6,6 (PA6,6). In the case of PP and HDPE, wetting coefficient evaluation predicts that the MWNTs should locate at the interface but the fraction of MWNTs which migrates from PET is only 7%. In the case of PVDF and PA6,6, the wetting coefficients predict that the MWNTs should stay in PET and the experimental results confirm this prediction. Li and Shimizu [19] have studied conductive cocontinuous blends of PVDF/polyamide 6 (PA6) filled with carbon nanotubes. The MWNTs were exclusively located in PA6 phase. Meincke et al. [20] have studied the properties of MWNTs filled PA6 and its blends with acrylonitrile/butadiene/styrene (ABS). The MWNTs were found to stay in the PA6 phase also creating a triple-continuous structure. Zou et al. [21] have

* Corresponding authors. Tel.: +32 10 478412; fax: +32 10 451593.
E-mail addresses: jacques.devaux@uclouvain.be (J. Devaux), christian.bailly@uclouvain.be (C. Bailly).
[1] Tel.: +32 10 47 3556.

0032-3861/$ – see front matter © 2010 Elsevier Ltd. All rights reserved.
doi:10.1016/j.polymer.2010.01.050

studied the morphology of poly(phenylene sulfide)/polyamide 6,6 blends with various amounts of acid treated MWNTs. It was observed that the MWNTs are preferentially located in the PA6,6 phase. In all these studies, the filler was found to concentrate in the more polar phase. As the filler was first added in the more favourable phase, it was not possible to determine if high aspect ratio nanoparticles are able to transport from one phase to the other one or to the interface. More recently, Pötschke et al. [22] have presented migration of MWNTs from HDPE concentrates to PC and PA. The MWNTs were well dispersed in the PC and PA matrix and electrical percolation was achieved at lower MWNTs contents as compared to direct incorporation. In another paper [23], Pötschke and coworkers have introduced MWNTs into blends of PC and poly(styrene acrylonitrile) (SAN) by melt mixing. In all blends, even when the MWNTs were first dispersed in SAN, the MWNTs were exclusively located in the PC phase despite the minor differences in the wetting behaviour between the two phases. The electrical resistivities were lower as compared to PC and SAN with the same MWNTs content. The authors explain the CNT transfer based on a theoretical work given by Krasovitsky and Marmur [24] concerning the penetration of particles with different aspect ratios into a liquid drop surrounded by another liquid. They show that particles with very high aspect ratio exhibit complete penetration into the better wetting liquid even for very small differences in the wetting behaviour. From those theoretical calculations, Pötschke and coworkers [23] concluded that the localization of very long particles at the interface is an instable transition state and thus highly improbable in the final blend morphology. Only particles oriented completely parallel to the interface may be jammed there. Bose et al. [25,26] have studied blends of PA6 and ABS in the presence of styrene-maleic anhydride copolymer (SMA) and MWNTs. The MWNTs appeared to locate at the interface because they were chemically coupled to the SMA compatibilizer, which locates at the interface. Wu et al. [27] have used functionalized MWNTs to control the morphology of immiscible poly(ε-caprolactone) (PCL) polylactide (PLA) blend. The MWNT were selectively localized in the PCL phase and part of them were at the interface between both polymers. The selective localization of MWNTs in PCL was attributed to the much higher viscosity of PLA and their presence at the interface was attributed to their functionalization. Indeed, the carboxylic groups on the MWNTs surface have a good affinity with both PCL and PLA. Unfunctionalized MWNTs were therefore not found at the interface in the same PCL/PLA blend.

The general mechanisms of particle migration inside a molten heterogeneous medium have been described [28,29]. Migration first implies that those particles approach the interface. Three mechanisms can be involved: Brownian motion, particle motion induced by shear and motion of particles which are trapped in the inter-droplet zone during a collision between two dispersed polymer drops. For silica particles, the Brownian motion contribution was estimated negligible. Indeed, the high viscosity of molten polymers hinders the Brownian particle motion. A global description of particle migration should also consider the surface effects. When a particle migrates from one polymer phase to the other, the adsorbed macromolecules must desorb to be replaced by macromolecules of the other polymer.

The location of MWNTs at the interface in a blend of two immiscible polymers has so far only been shown in very few specific examples where the MWNTs were previously modified [25–27]. In this paper, we demonstrate the possibility to jam unmodified MWNTs at the interface of an immiscible polymer blend of PA and ethylene–acrylate copolymer (EA) in a thermodynamically stable way. Moreover, we compare the theoretical predictions given by the wetting coefficient evaluation to the observed morphology.

2. Experimental part

2.1. Materials

The blends under study are composed of two types of immiscible polymers: two different grades of polyamide and a ethylene–acrylate copolymer. The two polyamides are PA6 (Durethan B40F, Bayer) on one hand and PA12 (Vestamid L2101F, Evonik Degussa AG) on the other hand. The ethylene–acrylate copolymer (EA) used is a random copolymer of ethylene and 26–30 wt.% methyl acrylate (Lotryl 28MA07, Arkema).

The MWNTs are Nanocyl®-7000 (Nanocyl S.A., Belgium) with a purity of 90%, produced via catalytic carbon vapor deposition (CCVD) process. They present 7 graphene shells, their average diameter is 9.5 nm and their average length is 1.5 μm according to the supplier. The carbon purity is 90% and the surface area is 250–300 $m^2 g^{-1}$.

The solvents used in this study are formic acid (purity 98+%, Acros Organics), *m*-cresol (purity 97%, Acros Organics), chloroform (Chloroform for HPLC stabilized with Amylene, Biosolve) and dimethylsulfoxyde (purity 99+%, Janssen Chimica).

2.2. Blends preparation

2.2.1. Melt compounding process

Blends of 90% of EA and 10% PA (w/w) with and without MWNTs have been prepared by mixing in a co-rotating twin-screw minicompounder (DSM Xplore Microcompounder 15 cm^3) with two stainless steel screws and a bypass allowing continuous recycling of the material at the head of the mixing chamber. Rotation speed and mixing time can be independently modified. Before melt compounding, the polymers have been dried for 24 h at 50 °C under vacuum.

2.2.2. Preparation conditions

The preparation conditions are reported in Table 1.

2.3. Characterization

2.3.1. Scanning electron microscopy (SEM)

Scanning electron microscopy has been performed on cryo-fractured surfaces using a LEO 982 (Zeiss).

2.3.2. Transmission electron microscopy (TEM)

The filler dispersion in nanocomposites has been examined using a LEO 922 Transmission Electron Microscope (TEM) operating at 200 kV.

The specimens are cut perpendicularly to the axes of the extruded samples using a Reichert Microtome. Ultrathin sections of approximately 95 nm in thickness are cut using a cryodiamond knife with a cut angle of 35° (Diatome, Switzerland) and collected in a blend of 60 vol% DMSO/40 vol% milliQ water on 400 mesh copper grids.

Table 1
Preparation parameters of the different composites.

	Mixing time min	Screw rotation speed rpm	Mixing temperature °C
PA6 + MWNTs	10	250	240
PA12 + MWNTs	10	250	240
EA + MWNTs	15	250	100
EA + PA6 + MWNTs	10	250	240
EA + PA12 + MWNTs	10	250	240

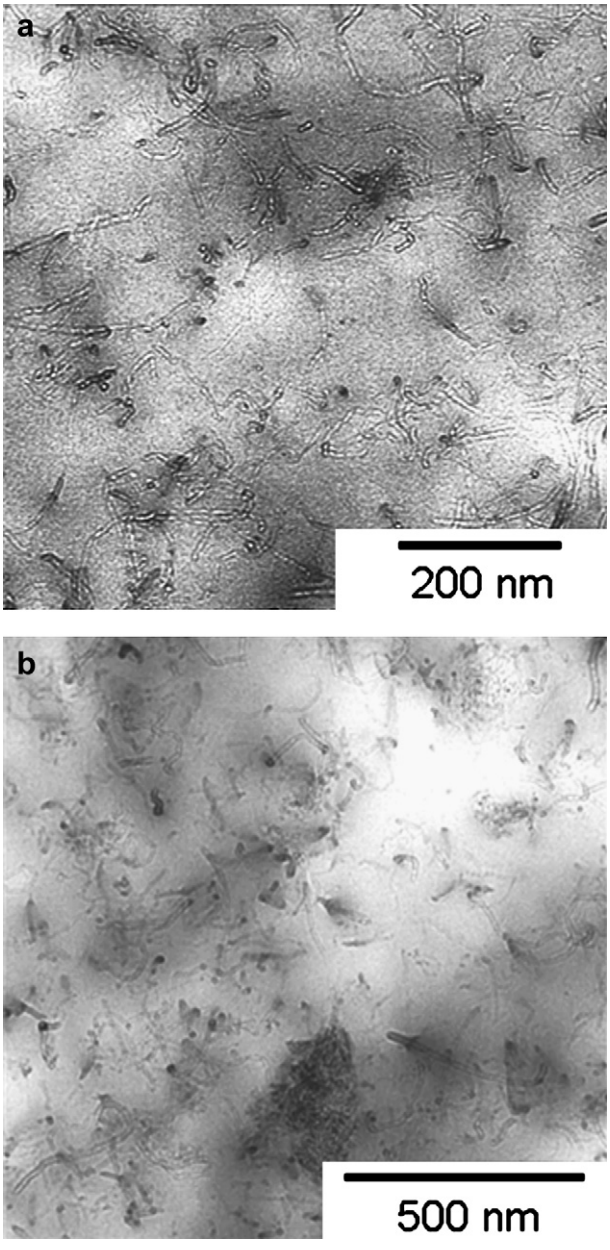

Fig. 1. TEM micrographs of PA containing 2 wt.%MWNTs (a) PA6 + 2 wt.%MWNTs, (b) PA12 + 2 wt.%MWNTs.

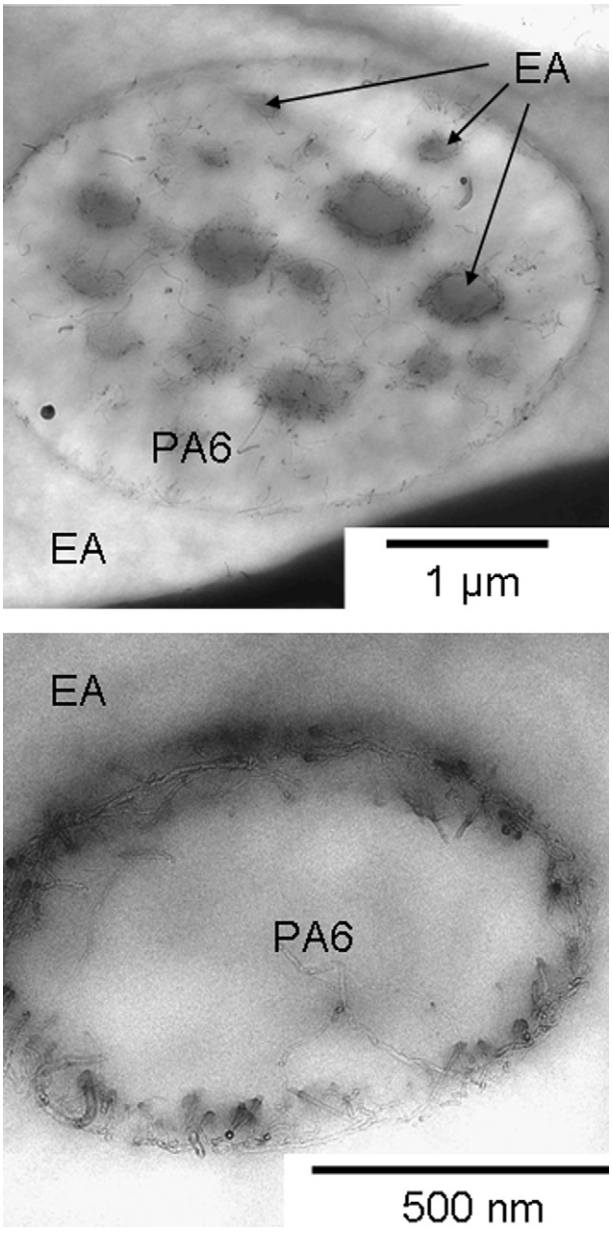

Fig. 2. TEM micrographs of a blend of 10 wt.% [PA6 + 2 wt.%MWNTs] – 90 wt.% EA.

2.3.3. Soxhlet

A Soxhlet device has been used to extract the MWNTs from the composite EA + 2 wt.%MWNTs. The extraction is performed using chloroform at 65 °C. Two different extraction durations are used: 24 h and 5 days. 50 mg EA + 2 wt.%MWNTs are deposited in the glass fibre thimble and the extraction using 300 ml chloroform is performed for the desired duration.

A control Soxhlet has also been done, 50 mg EA are deposited in the glass fibre thimble and the extraction with 300 ml chloroform has been performed for 5 days.

2.3.4. Under pressure filtration

Under pressure filtration has been performed with the help of a Sartorius SM 16249 pressurized filtration device supporting a maximum pressure of 10 bar and a maximum temperature of 150 °C. The maximum volume is of 220 ml. The solutions of PA and carbon nanotubes are filtered on Aluminium oxide membrane Anodisc 47 presenting a pore size of 0.1 μm (Whatman, England).

The PA6 + 2 wt.%MWNTs composite is first dissolved in formic acid at room temperature (~20 mg PA6 + 2 wt.%MWNTs in 40 ml formic acid). Next, the solution is sonicated for 2 h in a Bioblock Scientific type T700 (35 kHz). The solution is next filtrated using the under 4.8 bar pressure filtration device at room temperature. The suspension is next rinsed with either 80 ml solvent (PA6 + 2%MWNTs (2 rinses)) or 400 ml solvent (PA6 + 2%MWNTs (10 rinses)). In both cases, 80 ml formic acid is poured in the under pressure filtration device and no pression is applied for 15 min. Next, a pressure of 1 bar is applied to ensure a slow filtration. For PA6 + 2%MWNTs (10 rinses), these operations are repeated 5 times. After rinsing, the aluminium oxide membrane is rinsed with demineralised water. It is next dried on a hot plate at 80 °C for 1 night and the in a vacuum oven at 50 °C under vacuum.

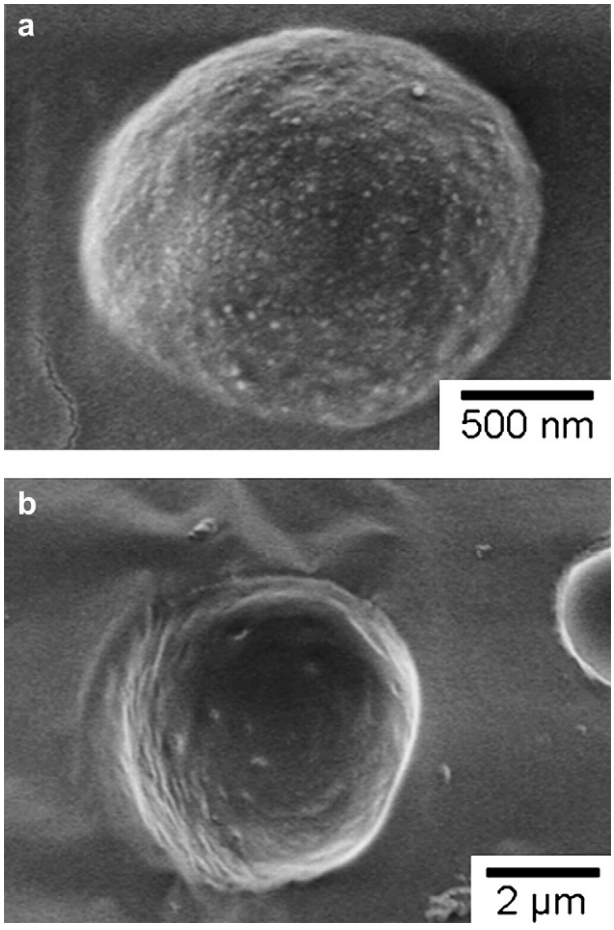

Fig. 3. SEM micrographs of a cryofracture of a blend of 10 wt.% [PA6 + 2 wt.%MWNTs] – 90 wt.% EA; (a) droplet of PA6; (b) cavity in the EA matrix.

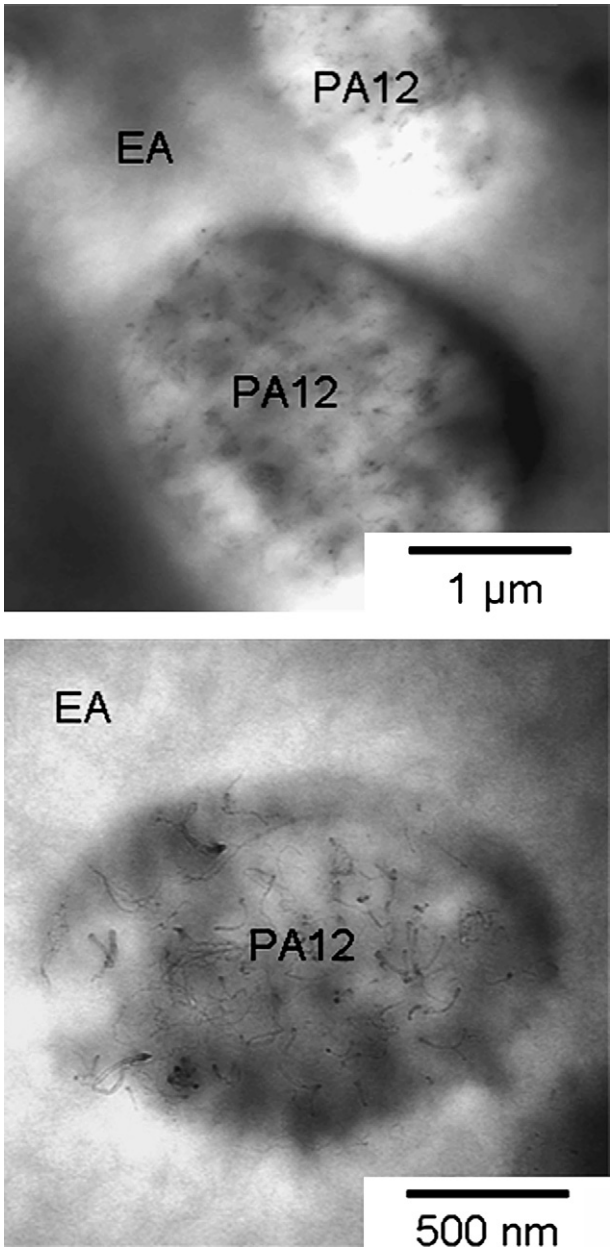

Fig. 4. TEM micrographs of a blend of 10 wt.% [PA12 + 2 wt.%MWNTs] – 90 wt.% EA.

A solution of pure PA6 in formic acid (~20 mg PA6 in 40 ml formic acid) is also filtrated on the aluminium membrane. The filtration is done under 4.8 bar. The membrane is next rinsed with 400 ml solvent without pressure to ensure a quite low rinsing. The membrane is next rinsed with demineralised water and dried on a hot plate at 80 °C overnight.

The PA12 + 2 wt.%MWNTs composite is dissolved in *m*-cresol at room temperature (~25 mg in 40 mL *m*-cresol). The solution is next sonicated for 2 h. The solution is next filtrated using the under pressure filtration device at 4.8 bar at room temperature. The membrane is next rinsed with either 80 ml solvent (PA12 + 2%MWNTs (2 rinses)) or 400 ml solvent (PA12 + 2%MWNTs (10 rinses)) under 4.8 bar. After rinsing, the aluminium oxide membrane is dried on a hot plate at 80 °C for 1 night and the in a vacuum oven at 50 °C under vacuum.

A solution of pure PA12 in *m*-cresol (~20 mg PA12 in 40 mL *m*-cresol) is also filtrated on the aluminium membrane under 4.8 bar. The membrane is next rinsed with 400 ml solvent under 1 bar to ensure slow filtration. The membrane is next rinsed with demineralised water and dried on a hot plate at 80 °C overnight.

2.3.5. Thermogravimetry analysis (TGA)

Thermogravimetry measurements have been performed with the help of a Mettler Toledo TGA/SDTA 851e under dry air with a flow rate of 50 mL/min. Samples are heated at 5 K/min and the relative mass loss of the samples is recorded from 298.15 to 1273.15 K.

Only the results between 373.15 K and 1073.15 K are presented here. The curves are therefore shifted to the same starting value at 373.15 K on a relative weight % scale.

2.3.6. Decantation tests

The nanocomposites PA6 + 2%MWNTs and PA12 + 2%MWNTs were dissolved in *m*-cresol (20 mg in 40 ml) at room temperature. For the comparison, as produced MWNT were milled during 30 min with the help of a vibrating mill (Perkin Elmer Vibrating mill (220 V, 50 Hz)) with a stainless steel capsule set. These MWNTs were next dispersed in *m*-cresol (0.4 mg in 40 ml) at room temperature. All the suspensions were next sonicated (Bioblock Scientific type T700 (35 kHz)) during 2 h in *m*-cresol, followed by centrifugation during different times. For the sonication, solutions of polymers and carbon nanotubes were poured in 2.0 ml Eppendorf Safe Lock Tubes and then centrifuged at 13400 rpm using a Mini-Spin Eppendorf centrifuge.

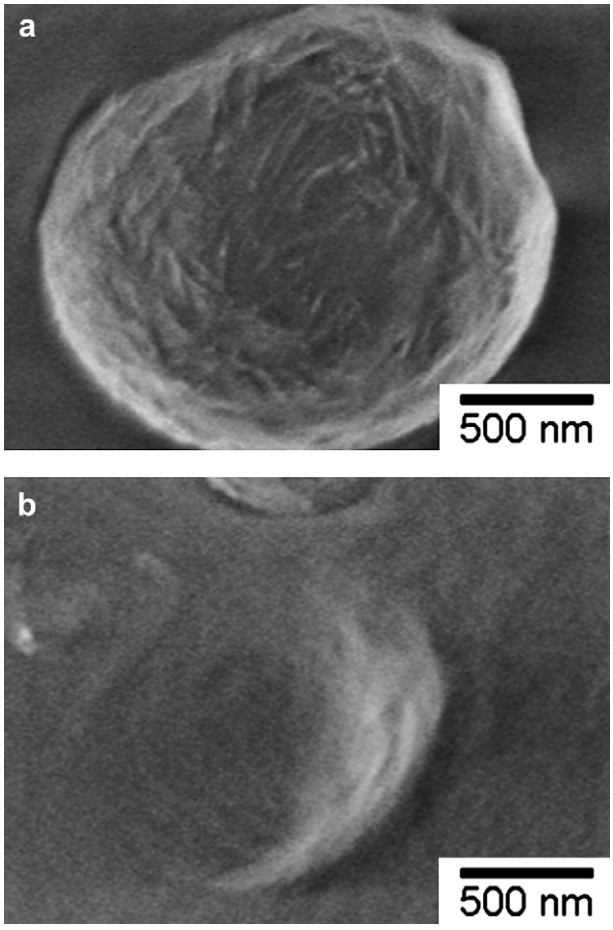

Fig. 5. SEM micrographs of a cryofracture of a blend of 10 wt.% [PA12 + 2 wt.%MWNTs] – 90 wt.% EA; (a) droplet of PA12; (b) cavity in the EA matrix.

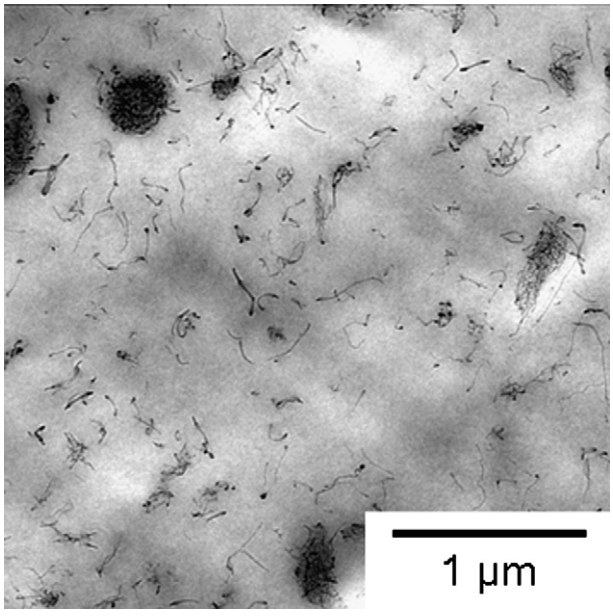

Fig. 6. TEM micrograph nanocomposites based on EA containing 2 wt.%MWNTs (EA + 2 wt.%MWNTs).

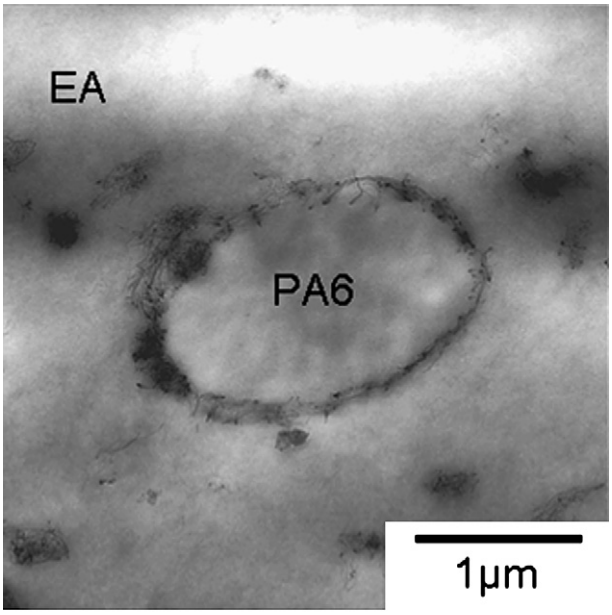

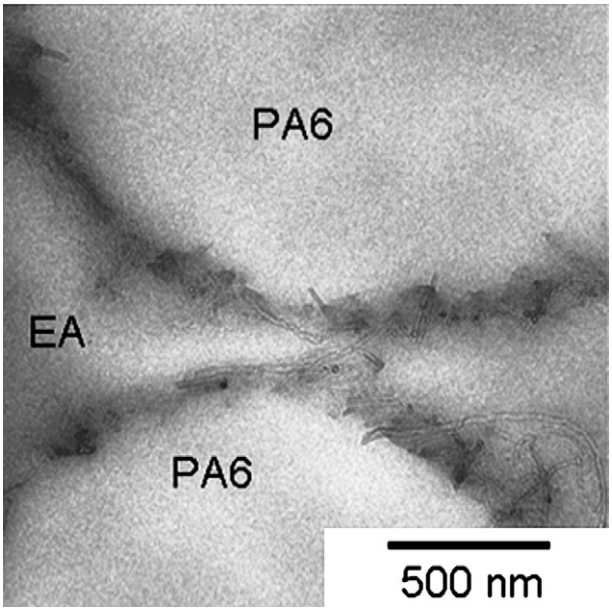

Fig. 7. TEM micrographs of a blend of 10 wt.% PA6 – 90 wt.% [EA + 2 wt.%MWNTs].

3. Results and discussion

3.1. Blend morphology and nanotube localization

We use three different methods to mix the MWNTs with the two immiscible polymers. First, the MWNTs are added to PA before mixing with EA (Method 1: Premixing in PA). Second, the MWNTs are added to EA before mixing with PA (Method 2: Premixing in EA). Finally, the three components are simultaneously mixed (Method 3: Simultaneous mixing).

3.1.1. Method 1: premixing in PA

When the MWNTs are first mixed with PA (PA + 2 wt.%MWNTs), their distribution is homogeneous. The MWNTs are mainly individualized but some aggregates of MWNTs remain in PA12 (Fig. 1).

When this composite is next mixed with EA (10 wt.% [PA + 2 wt.%MWNTs] – 90 wt.% EA), a morphology of PA droplets, containing EA sub-inclusions, dispersed in an EA matrix is

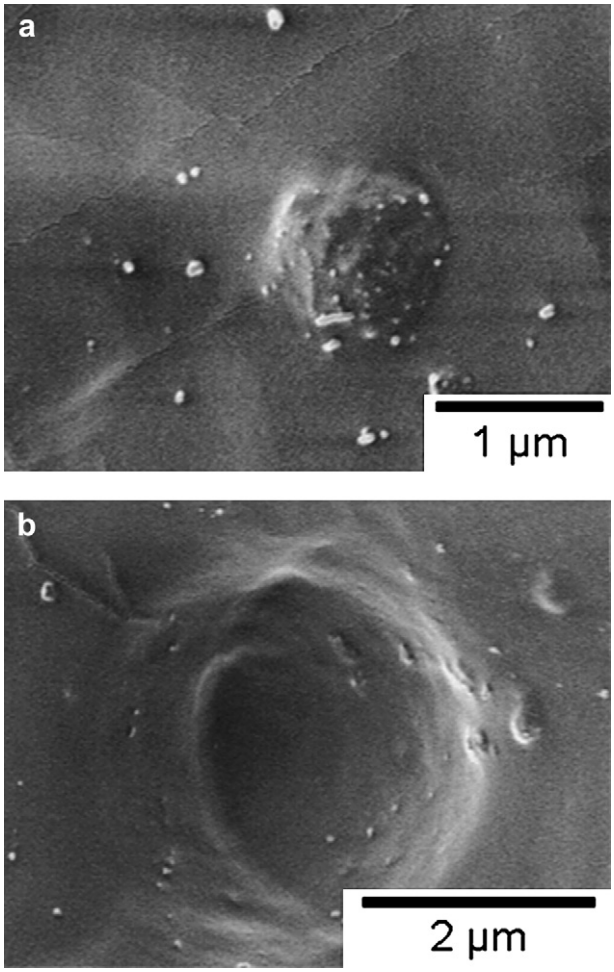

Fig. 8. SEM micrographs of a cryofracture of a blend of 10 wt.% PA6 – 90 wt.% [EA + 2 wt.%MWNTs]; (a) droplet of PA; (b) cavity in the EA matrix.

obtained. When the PA used is a PA6, although some MWNTs stay in the PA droplets, most of them migrate to the interface between the polymers (Fig. 2). SEM micrographs of cryofractured samples of the same blend (Fig. 3) display the surface of PA nodules and the cavities in the matrix due to PA droplets removal after cryofracture. The figure shows that although the MWNTs are at the interface of the blend, they are more embedded in the PA6 phase and no MWNTs are present in the EA matrix. When the PA used is PA12, the MWNTs stay well dispersed in the PA phase as shown on TEM micrographs (Fig. 4). SEM micrographs of the same blend demonstrate that the MWNTs are localized in the PA nodules since no MWNTs are pulled out of the interface or in the EA (Fig. 5). This is in good agreement with the morphology observed by TEM. It is also important to note that the selective localization of MWNTs is stable. The same morphologies are observed even after 60 min of mixing.

3.1.2. Method 2: premixing in EA

When mixed in EA (EA + 2 wt.%MWNTs), the MWNTs are not so well dispersed as in PA. Small aggregates are still present after compounding (Fig. 6).

When the premix of EA and MWNTs is further blended with PA (10 wt.% PA – 90 wt.% [EA + 2 wt.%MWNTs]), a morphology of PA nodules dispersed in a matrix of EA is obtained. For both polyamides, some MWNTs aggregates are still present in the EA matrix but most of the MWNTs migrate to the interface between the two polymers. When PA6 is used, the MWNTs are jammed at the interface (Fig. 7). The MWNTs are localized at the interface between

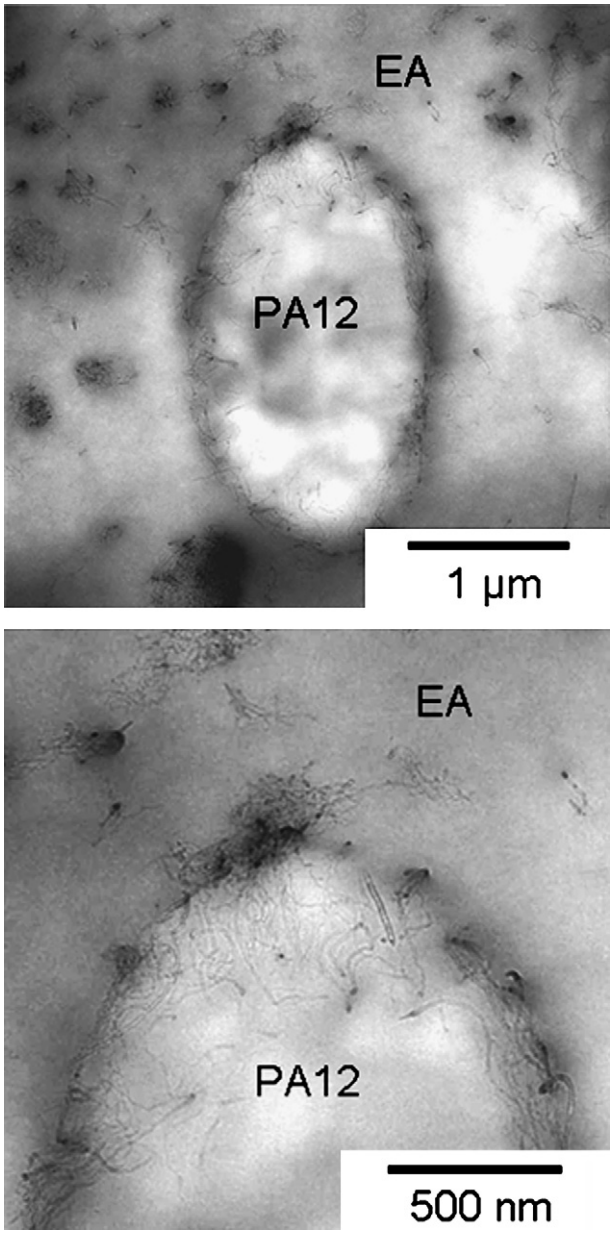

Fig. 9. TEM micrographs of a blend of 10 wt.% PA12 – 90 wt.% [EA + 2 wt.%MWNTs].

the polymers. They are present at the surface of the nodules and in the cavities remaining in the matrix after cryofracturing (Fig. 8). However, when PA12 is used, some parts of the MWNTs are jammed at the interface and some parts penetrate inside the PA nodules (Fig. 9). On SEM micrographs (Fig. 10), MWNTs seem "attached" to the PA nodules. They are present at the interface but only at the surface of the PA nodules. No MWNTs are visible in the EA matrix. The same kind of morphology is observed for 60 min mixing, indicating that the situation is stable.

3.1.3. Method 3: simultaneous mixing

When the three components are simultaneously mixed, the carbon nanotubes are preferentially located at the interface between both polymers although some MWNTs can be seen in the PA nodules when PA12 is used. The behaviour observed using this dispersion method is the same as when MWNTs are premixed with EA (method 2). This result is firstly explained by the large amount of EA present in the system as compared to PA. The probability for the

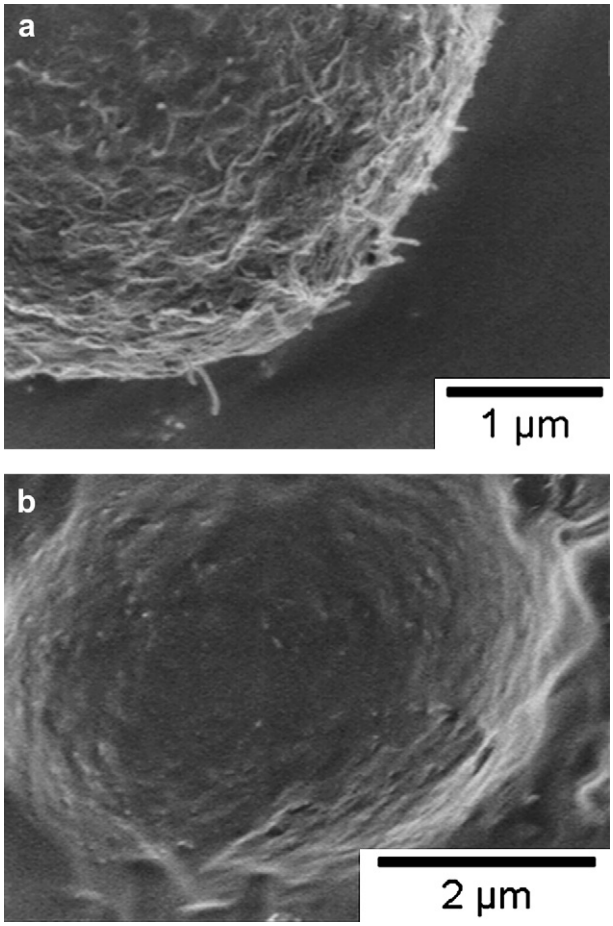

Fig. 10. SEM micrographs of a cryofracture of a blend of 10 wt.% PA12 – 90 wt.% [EA + 2 wt.%MWNTs]; (a) droplet of PA; (b) cavity in the EA matrix.

MWNTs to first meet EA is thus higher than the probability to first meet PA. Secondly, PA and EA exhibit very different melting points. The melting temperature of PA 6 is around 220 °C, of PA12 around 180 °C and of EA around 65 °C. The ethylene–acrylate copolymer is therefore molten before PA and is thus the first polymer to "wet" the MWNTs. The morphology is thus mainly similar to the morphology observed with method 2.

3.2. Wetting coefficient analysis

Classical thermodynamics is often used to predict the position of fillers in blends of immiscible polymers. In the equilibrium state, the location of a filler in a polymer blend can be predicted by the minimization of the interfacial energy. According to Young's equation, it is possible to find the equilibrium position of the filler by evaluating the wetting coefficient ω_a [30].

Table 2
Surface energies at 20 °C, polar fractions and temperature coefficients for poly(-ethylene) and poly(methyl acrylate).

Material	Total surface energy mJ m^{-2}	Dispersive surface energy, γ^d mJ m^{-2}	Polar surface energy, γ^p mJ m^{-2}	Polar fraction	Temperature coefficient
PMA	41	29.7	10.3	0.25122	−0.077
PE	35.7	35.7	0	0	−0.057

Table 3
Surface energies of the polymers and MWNT at 240 C.

Material	Total surface energy mJ m^{-2}	Dispersive surface energy, γ^d mJ m^{-2}	Polar surface energy, γ^p mJ m^{-2}
MWNT	27.8	17.6	10.2
EA	23.3	22.5	0.8
PA6	37.7	27.2	10.6
PA12	26.4	23.2	3.2

$$\omega_a = \frac{\gamma_{C-Pol\ B} - \gamma_{C-Pol\ A}}{\gamma_{Pol\ A-Pol\ B}} \quad (1)$$

where $\gamma_{C-Pol\ A}$, $\gamma_{C-Pol\ B}$, $\gamma_{Pol\ A-Pol\ B}$ are the interfacial energy respectively between MWNTs and polymer A, between MWNTs and polymer B and between polymer A and polymer B. If the wetting coefficient is higher than 1, the filler will preferentially be located in polymer A; if the wetting coefficient is lower than −1, the filler will preferentially be located in polymer B, and if the wetting coefficient is between −1 and 1, the filler will be located at the interface between the two polymers.

The interfacial energy can be evaluated from the surface energies of the components. Two main approaches can be used depending on the type of surfaces: the harmonic mean equation and the geometric mean equation. The harmonic mean equation (Equation (2)) is valid between low-energy materials and the geometric mean equation (Equation (3)) is valid between a low-energy material and a high energy material:

Harmonic mean equation:

$$\gamma_{12} = \gamma_1 + \gamma_2 - 4\left(\frac{\gamma_1^d\gamma_2^d}{\gamma_1^d + \gamma_2^d} + \frac{\gamma_1^p\gamma_2^p}{\gamma_1^p + \gamma_2^p}\right) \quad (2)$$

Geometric mean equation:

$$\gamma_{12} = \gamma_1 + \gamma_2 - 2\left(\sqrt{\gamma_1^d\gamma_2^d} + \sqrt{\gamma_1^p\gamma_2^p}\right) \quad (3)$$

where γ_1, γ_2 are the surface tensions of components 1, 2; γ_1^d, γ_2^d are the dispersive parts of the surface tensions of components 1, 2; and γ_1^p, γ_2^p are the polar parts of the surface tension of components 1, 2.

The values of the surface energy of polymers in the melt state have been extrapolated from literature values at 20 °C as detailed below and are summarized in Table 2, with the simplifying hypothesis that the polarity is independent of temperature. The surface tension for EA has been found by using an arithmetic mean value adapted to random copolymers (Equation (4)). The surface energy of EA is hence evaluated using the values of poly(ethylene) and poly(methyl acrylate) in the following way:

$$\gamma = x_{PE}\gamma_{PE} + x_{PMA}\gamma_{PMA} \quad (4)$$

Table 4
Interfacial energies as calculated using harmonic and geometric mean equations at 240 C.

Materials	Interfacial energy according to harmonic mean equation mJ m^{-2}	Interfacial energy according to geometric mean equation mJ m^{-2}
EA/PA6	8.8	5.7
EA/PA12	5.3	3.3
EA/MWNT	8.6	5.5
PA6/MWNT	2.0	1.0
PA12/MWNT	4.5	2.8

Table 5
Wetting coefficient evaluated according harmonic mean equation, geometric mean equation.

Materials	Wetting coefficient according to harmonic mean equation	Wetting coefficient according to geometric mean equation	Prediction
EA/PA6/MWNT	−0.7	−0.8	Interface
EA/PA12/MWNT	−2.9	−4.0	PA12

where x_{PE} and x_{PMA} are the molar fractions and γ_{PE} and γ_{PMA} are the surface tensions of respectively poly(ethylene) and poly(methyl acrylate).

The EA used is a random copolymer of ethylene and 26–30 wt.% methyl acrylate. The mean value of 28 wt.% methyl acrylate was used. The molar fractions were therefore evaluated as 14% PMA and 86% PE. The values of the surface energies for both components at 20 °C are given in Table 2. The values at 240 °C were evaluated based on the values at 20 °C, using the temperature coefficient for each component.

The temperature dependence of the surface tensions of PA6 and PA12 was not found in the literature. The temperature dependence has therefore been approximated by the one of PA66 ($-d\gamma/dT = 0.065$ mN m^{-1} °C^{-1}) [30] due to the similar chemical structure. The polarity of PA6 has been evaluated by Son [31] to be 0.28. The surface tension and the polarity of PA12 have been taken from literature [32–34].

Owing to the difficulty to measure interactions between carbon nanotubes and polymer liquids, data concerning the surface tension and polarity of carbon nanotubes are limited. Barber et al. [35] have measured the static and dynamic wetting characteristics of individual MWNTs grown by arc-discharge and exhibiting a diameter of about 20 nm. They have used atomic force microscopy and a Wilhelmy balance to quantify the contact angle between various liquids and the carbon nanotubes. The total surface tension measured is 27.8 mJ m^{-2} with dispersive and polar components respectively equal to 17.6 mJ m^{-2} and 10.2 mJ m^{-2}. Nuriel et al. [36] have measured the surface tension of MWNTs with a diameter of approximately 30 nm. They have used electron microscopy to measure the contact angle between MWNTs and PP or PE glycol. A total surface energy of 45.3 mJ m^{-2} has been found with dispersive and polar components of respectively 18.4 mJ m^{-2} and 26.9 mJ m^{-2}. Their conclusion is however that the polar component should actually be lower than the measured values.

The MWNTs used in this study are unfunctionalized and should present a low polarity as compared to the MWNTs studied by Barber et al. [35] and especially by Nuriel et al. [36] The values of the surface energies of MWNTs measured by Barber et al. are shown in Table 3. From these values, the calculated interfacial energies between the polymers and the MWNTs are reported in Table 4.

Setting polymer A as EA, polymer B as PA in Equation (1), it is possible to evaluate the wetting coefficients for the two blends. Table 5 presents the values of this coefficient according to the harmonic mean or the geometric mean equations and the resulting predictions.

According to the values presented in Table 5, the MWNTs should locate at the interface in the EA/PA6 systems and in PA12 in the EA/

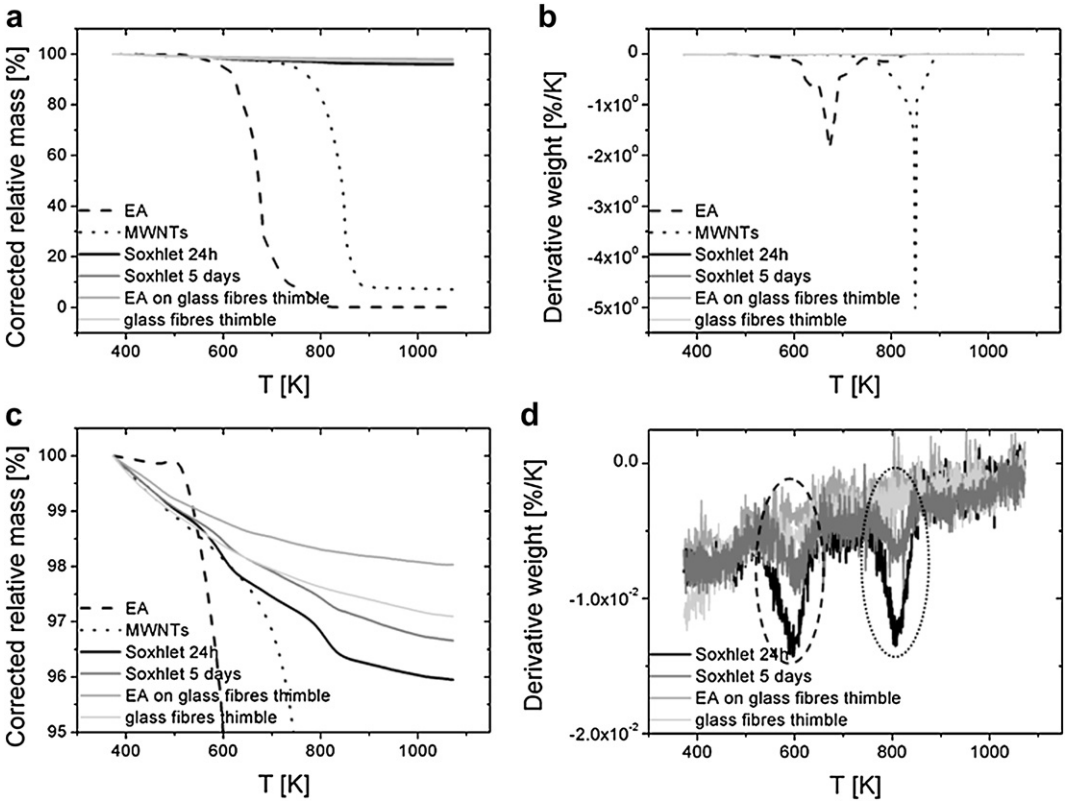

Fig. 11. Weight loss curves presenting (a) the relative mass, (b) the derivative weight and (c) relative mass for high mass fractions, versus the temperature for pure EA, pure MWNTs, the glass fibres containing the MWNTs extracted from the composite EA + 2%MWNTs using a Soxhlet during 24 h or 5 days, the glass fibre thimble after EA extraction for 5 days and the pure glass fibre thimble; (d) derivative weight versus sample temperature for the glass fibres containing the MWNTs extracted from the composite EA + 2%MWNTs using a Soxhlet during 24 h or 5 days, the glass fibre thimble after EA extraction for 5 days and the pure glass fibre thimble (dashed oval: polymer degradation, dotted oval: carbon nanotubes degradation).

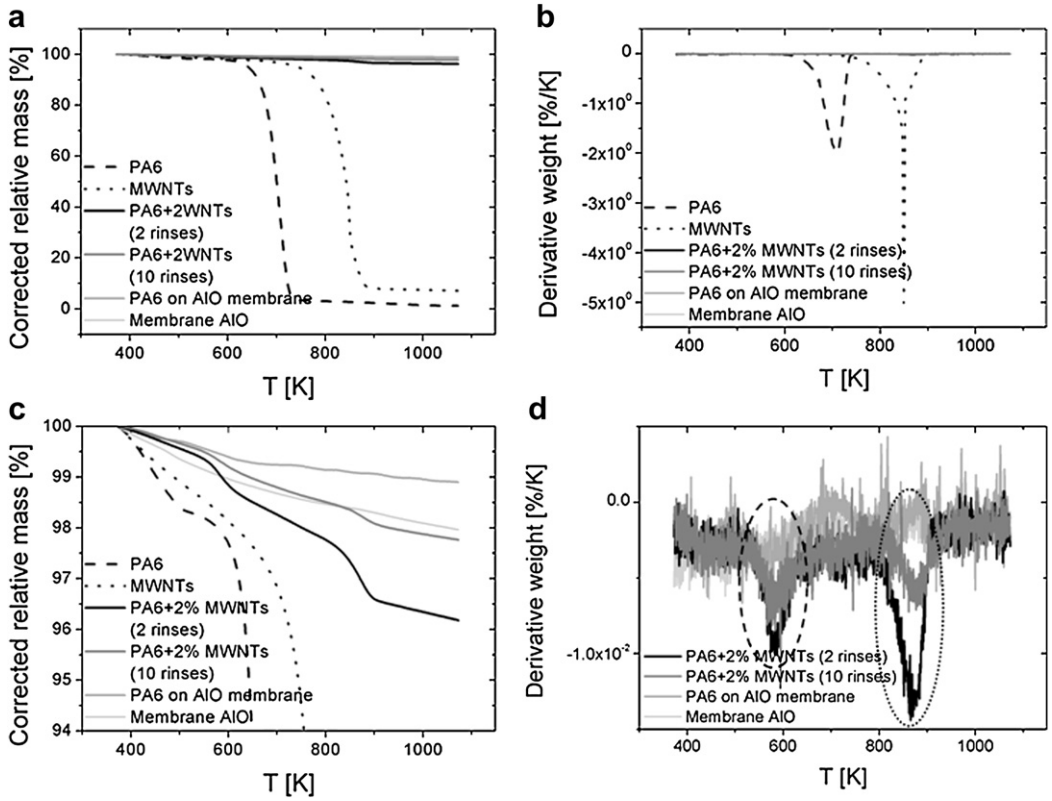

Fig. 12. Weight loss curves presenting (a) the relative mass, (b) the derivative weight and (c) relative mass for high mass fractions, versus the temperature for pure PA6, pure MWNTs, the aluminium oxide membrane containing the MWNTs extracted from the composite PA6 + 2%MWNTs using an under filtration device (see experimental section for more information) (PA6 + 2%MWNTs (2 rinses); PA6 + 2%MWNTs (10 rinses)), the aluminium oxide membrane after PA6 filtration and the pure aluminium oxide membrane; (d) derivative weight versus sample temperature for the glass fibres aluminium oxide membrane containing the MWNTs extracted from the composite PA6 + 2%MWNTs using an under filtration device (see experimental section for more information) (PA6 + 2%MWNTs (2 rinses); PA6 + 2%MWNTs (10 rinses)), the aluminium oxide membrane after PA6 filtration and the pure aluminium oxide membrane (dashed oval: polymer degradation, dotted oval: carbon nanotubes degradation).

PA12 system. The wetting coefficients have also been evaluated according to Nuriel et al. [36] predictions for the surface energy of the MWNTs. In this latter case, due to the high polar component of the surface energy, the predicted position of the MWNTs is in the PA phase whatever the PA used. However, these predictions must be handled with caution due to uncertainties concerning the surface energies of both polymers and carbon nanotubes. To some extent, it is possible to assess how the uncertainties on the total surface energy of MWNTs affect the prediction. Considering the presence of 1% oxygen on the MWNTs and accepting that the oxygen atoms are exclusively located on the outer shell, we can evaluate a maximum oxygen fraction to be about 5.5% on the outer shell. The polarity of the MWNTs can thus be roughly estimated at the order of 5% also. The lowest value of total surface energy found in the literature is 27.8 mJ/m^2. The theoretical estimation for the surface tension for single shell carbon nanotubes varies from 40 to 80 mJ/m^2 [36–38]. Thus, we can consider a total surface energy varying between 27.8 and 80 mJ/m^2. The prediction based on the evaluation of the wetting coefficient is unchanged for PA6/EA blends. The prediction is more sensitive in the case of PA12/EA blends. In this latter case, for the above mentioned conditions, the prediction of a localization in PA12 is found for a total surface energy higher than 47 mJ/m^2.

However, the final morphology is also depending on the mixing strategy. When PA6 is used, the MWNTs are localized at the interface when they are premixed in EA or during simultaneous mixing but they remain in the PA phase when they are premixed in PA. When PA12 is used, the MWNTs remain well dispersed in PA when they are premixed in PA but they migrate to the interface when they are premixed in EA or during simultaneous mixing. Our results thus show that thermodynamics based on surface tensions of the neat polymers and as produced MWNTs is not sufficient to predict the localization of the MWNTs in the polymer blends under study here.

3.3. Polymer adsorption on the carbon nanotubes

The observed morphology of the nanocomposite is not only depending on the polyamide used but also on the mixing sequence. This dependence can be explained either by kinetics effects if the system has not reached its equilibrium state or by a modification of interfacial thermodynamics during early stages of mixing. The observed morphologies are stable even after 60 min mixing, indicating that the mixing sequence influence is not linked to a kinetic effect. There should be a modification of the surface properties of the MWNTs and thus of interfacial thermodynamics during the premixing step (method 1 and 2) or during the early stages of compounding (method 3).

Srebnik and coworkers [39,40] have used Monte Carlo simulations to suggest that weakly attractive van der Waals forces are sufficient to induce polymer helical wrapping around MWNTs. Semiflexible polymer chains adsorb in the form of single or multiple helices while flexible chains adopt a random coil 'cloud' conformation around the tubes.

We have checked the adsorption of both polymers on the MWNTs surface by different methods. First, the presence of adsorbed EA is evidenced using TGA. Next the adsorption of PA is demonstrated using TGA and decantation tests.

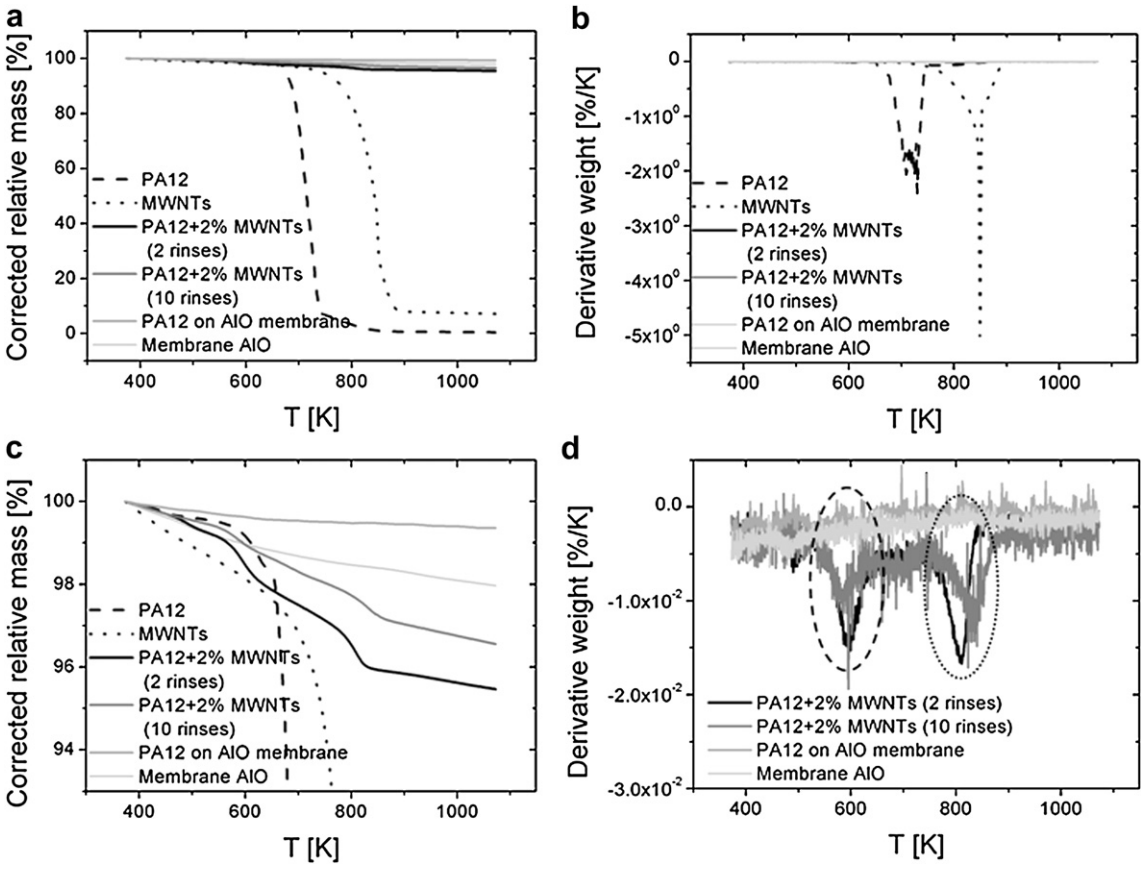

Fig. 13. Weight loss curves presenting (a) the relative mass, (b) the derivative weight and (c) relative mass for high mass fractions, versus the temperature for pure PA12, pure MWNTs, the aluminium oxide membrane containing the MWNTs extracted from the composite PA12 + 2%MWNTs using an under filtration device (see experimental section for more information) (PA12 + 2%MWNTs (2rinses); PA12 + 2%MWNTs (10 rinses)), the aluminium oxide membrane after PA12 filtration and the pure aluminium oxide membrane; (d) derivative weight versus sample temperature for the glass fibres aluminium oxide membrane containing the MWNTs extracted from the composite PA12 + 2%MWNTs using an under filtration device (see experimental section for more information) (PA12 + 2%MWNTs (2 rinses); PA12 + 2%MWNTs (10 rinses)), the aluminium oxide membrane after PA12 filtration and the pure aluminium oxide membrane (dashed oval: polymer degradation, dotted oval: carbon nanotubes degradation).

3.3.1. EA adsorption

The MWNTs are extracted from an EA nanocomposite containing 2 wt.%MWNTs with the help of a Soxhlet with boiling chloroform. Due to their short size after extrusion, the MWNTs are retained between the fibres in the glass fibres thimble. To check the polymer extraction kinetics, Soxhlet have been performed for one day and 5 days. A Soxhlet with virgin EA is made under the same conditions for comparison.

3.3.1.1. Thermogravimetric analysis (TGA). Fig. 11 presents the TGA analysis under dry air for the glass fibres retaining the MWNTs from the composite EA + 2 wt.%MWNTs (Soxhlet 24 h, Soxhlet 5 days), the glass fibres thimble after extraction of pure EA for 5 days (EA on glass fibre thimble), the pure glass fibres thimble (glass fibres thimble), the pure EA (EA) and the as produced MWNTs (MWNTs). The overall relative mass and derivative weight are presented on Fig. 11a and b to assess the degradation steps of the polymer and the MWNTs. Fig. 11c clearly shows two weight loss transitions for the MWNTs extracted from the composite (Soxhlet 24 h and Soxhlet 5 days). The first one, around 600 K, is attributed to the presence of adsorbed polymer while the second one, over 800 K, is attributed to the MWNTs oxidation under air atmosphere. These two weight losses are highlighted in Fig. 11d, which represents the derivative of weight versus temperature. The peaks linked to the polymer degradation are surrounded with a dashed oval and the peaks linked to the MWNTs degradation are surrounded with a dotted oval. It is worth noting that no significant weight loss is observed for the glass fibres after EA extraction for 5 days. The polymer degradation peaks observed for both Soxhlet 24 and Soxhlet 5 days are thus not due to polymer chains sticking to the glass fibres but to adsorption on the MWNTs. Although it is impossible to get fully quantitative analysis of the amount of adsorbed polymer due to the presence of a large amount of glass fibres, we can conclude that the weight of the adsorbed polymer is nearly equivalent to the weight of MWNTs. This evaluation is consistent for both extraction times, 24 h and 5 days, indicating that this polymer is adsorbed and further washing will not remove it. It is clear that such an amount of polymer represents the

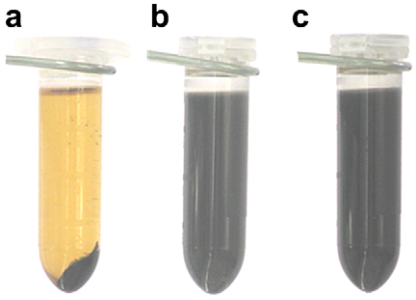

Fig. 14. Decantation tests after centrifugation; (a) milled MWNTs dispersed in *m*-cresol; (b) composite of PA6 containing MWNTs dissolved in *m*-cresol; (c) composite of PA12 containing MWNTs dissolved in *m*-cresol.

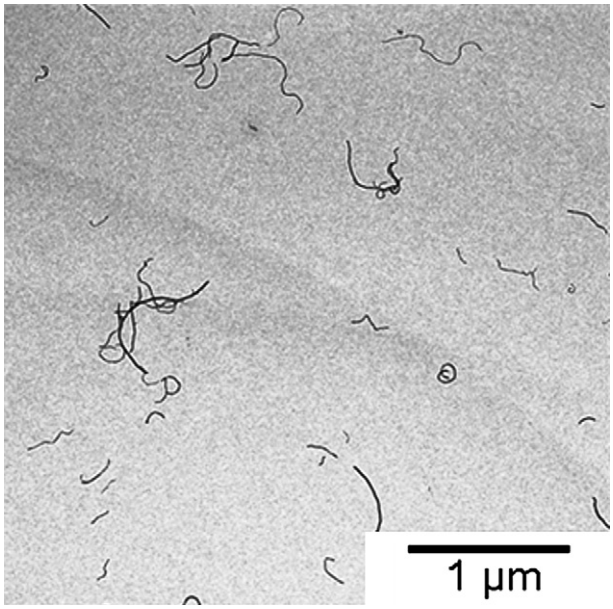

Fig. 15. TEM micrograph of the MWNTs extracted from PA6 using *m*-cresol.

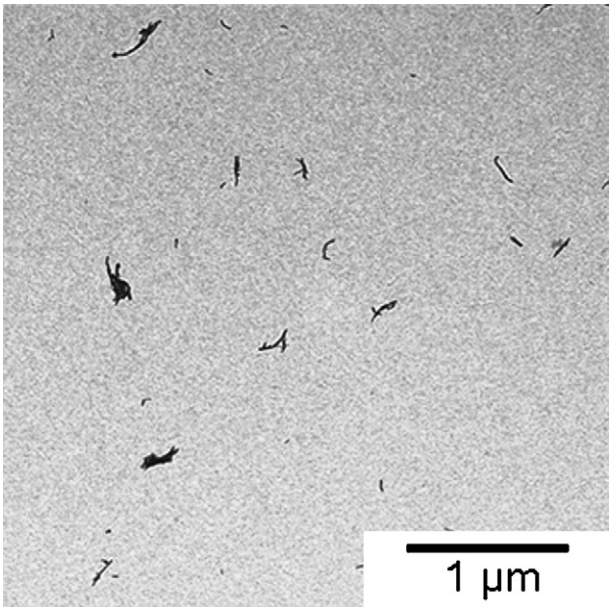

Fig. 17. MWNTs milled 30 min in a vibrating mill.

adsorption of more than one monolayer. This is likely due to tight entanglements between adsorbed chains and non-adsorbed chains.

3.3.2. PA adsorption

The adsorption of both PA6 and PA12 is proved by thermogravimetric analysis on MWNTs extracted from PA and decantation tests.

3.3.2.1. Thermogravimetric analysis (TGA). Polyamide adsorption is first proved by under pressure filtration experiments combined with TGA. The details of the separation procedure are given in the Experimental Section. Besides aluminium membrane containing MWNTs extracted from PA6 and PA12, also the pure polymers, the neat MWNTs, a clean aluminium oxide membrane and an aluminium oxide membrane after filtration of a solution of pure PA are also analyzed by TGA as controls. Figs. 12 and 13 present the relative mass loss and the derivative weight vs. temperature for the PA based systems. Figs. 12c and 13c present the relative mass for high mass fractions. Both figures show a first mass loss around 600 K which is attributed to the presence of polymer adsorbed on the MWNTs and a second mass around 850 K which is attributed to the oxidation of the MWNTs. As highlighted on Figs. 12d and 13d, the mass loss due to the adsorbed polymer is present after 2 rinses as well as 10 rinses in approximetly the same ratios, indicating that polymer is adsorbed in a partially irreversible way. However, for the PA6 based systems, due to the high background and the low mass losses observed, it is difficult to claim that no polymer adsorbs on the aluminium oxide membrane. Decantation tests have therefore be done as a complementary indirect proof of PA adsorption.

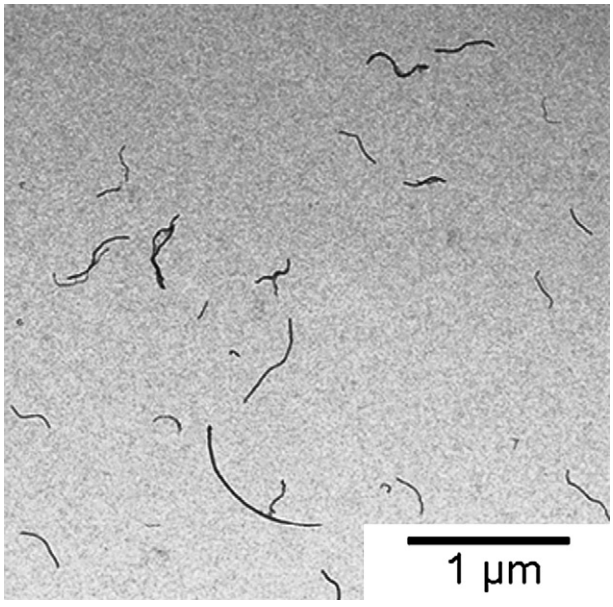

Fig. 16. TEM micrograph of the MWNTs extracted from PA12 using *m*-cresol.

3.3.2.2. Decantation tests. As it is not possible to fully exclude that part of the observed adsorption occurs on the aluminium membrane, the presence of adsorbed PA is also demonstrated by decantation tests. After sonication, the solutions containing

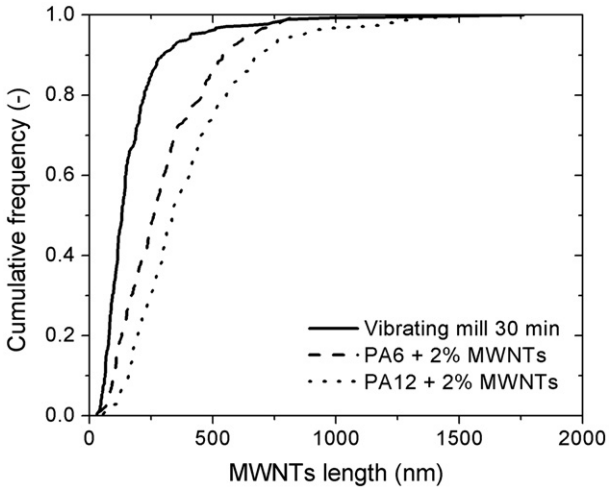

Fig. 18. Cumulative frequency of MWNTs from vibrating mill 30 min and from PA versus the MWNTs length.

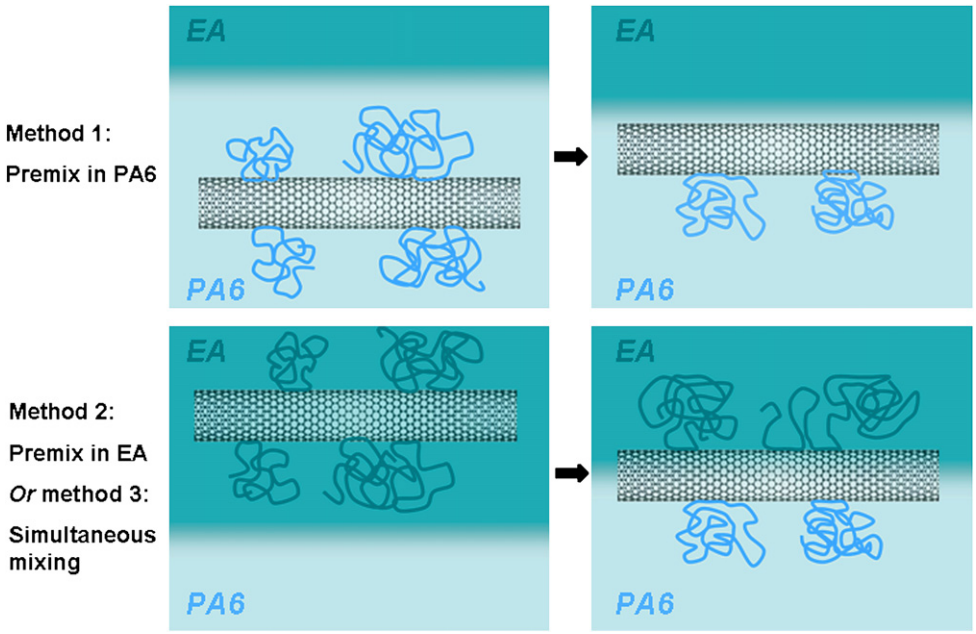

Fig. 19. Description of the migration mechanisms in the blend of EA, PA6 and MWNTs. It is impossible to know if there are chains adsorbed on MWNTs on EA side after migration in Method 1.

MWNTs were centrifugated during different times. After less than 1 min, the milled MWNTs migrate towards the bottom of the flask (Fig. 14a). The MWNTs from the composite PA6 + 2 wt.%MWNTs (Fig. 14b) and the composite PA12 + 2 wt.%MWNTs (Fig. 14c) partially migrate after 150 min but most of them are still in suspension even after at least 450 min centrifugation.

The sedimentation speed v for particles can be evaluated using Equation (5):

$$v = \frac{\omega^2 R\left(\gamma_{\text{particles}} - \gamma_{\text{solvent}}\right) d_p^2}{18\mu} \tag{5}$$

with ω the angular speed, R the centrifuge radius, γ the surface tension, d_p the equivalent particule diameter and μ the solvent viscosity. It is directly proportional to the square of the equivalent diameter of the particles. The size of the MWNTs, either extracted from polymer after extrusion in PA6 (Fig. 15) or PA12 (Fig. 16) or after 30 min milling in a vibrating mill (Fig. 17), has been measured by TEM (Fig. 18). The MWNTs extracted from PA6 and PA12 are nearly individualized. As presented in Fig. 18, the milled MWNTs are shorter than the extracted MWNTs but some aggregates are present (Fig. 17).

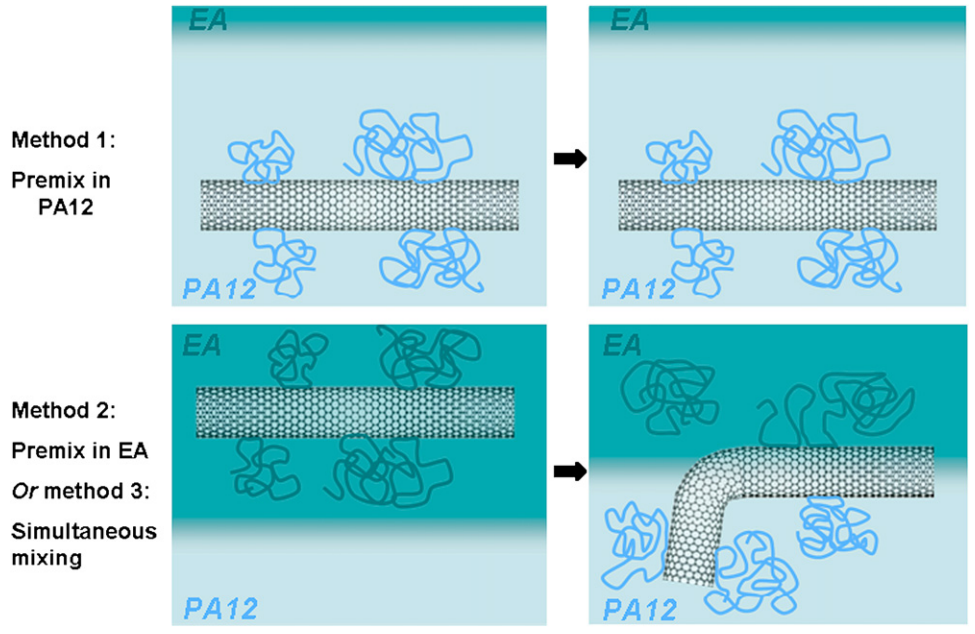

Fig. 20. Description of the migration mechanisms in the blend of EA, PA12 and MWNTs.

Because the aspect ratio and aggregation are different between the samples, the equivalent diameter of the nanoparticles is evaluated depending on the morphology. The nanotubes extracted from PA6 and PA12 are considered as cylinders presenting a diameter of 10 nm. The equivalent spherical diameter is evaluated to keep the same ratio surface-volume (Equation (6)). The equivalent diameter for MWNTs extracted from PA6 and PA12 is close to 14.8 nm.

$$d_p = \frac{3d_c l_c}{2l_c + d_c} \quad (6)$$

For the milled MWNTs, two extreme cases are considered: isotropic aggregates and anisotropic aggregates or cylinders. When isotropic aggregates are considered, the average diameter of the particles is 176.7 nm. When anisotropic aggregates are considered, Equation (6) is used, leading to an equivalent diameter of 65.7 nm. The sedimentation speed for MWNTs extracted from the composites is thus predicted to be 20–143 times lower than the sedimentation speed of the milled MWNTs, depending on the morphology assumption. Theoretically, the centrifugation time of MWNTs from composites should therefore vary from 20 to about 140 min. The actual decantation results show that while a small fraction of the MWNTs have indeed decanted during this time range, most of them are still in suspension even for much longer centrifugation times. The MWNTs thus remain in suspension due to the adsorption of PA on their surface and not to their very small size.

3.3.3. *Adsorption mechanism*

The mechanisms of adsorption of polymers on MWNTs have been widely studied for the non-covalent functionalization of MWNTs [41] and to improve their dispersion in organic solvents [42]. Some specific polymers presenting either ionic groups or an electron-rich backbone have already been shown to wrap around SWNTs. In the absence of chemical bonding between carbon particles and polymers, the origin of the interactions is electrostatic and/or Van der Waals. Xie and Soh [43] have attributed the association of carbon nanotubes and amylose to non specific van der Waals forces. Baskaran et al. [44] have demonstrated that the coating or wrapping of MWNTs is a general phenomenon occurring between polymers and MWNTs. They show that coating occurs irrespective of the nature of the polymers used. This phenomenon is attributed to non-covalent and non specific molecular interactions between CH groups on polymers and MWNTs, leading to polymer adsorption. A few percent of polymeric adsorbents could not be removed by washing, indicating the presence of partial irreversible coating. The authors also explain that adsorption is better in the case of melt blending or shear mixing than in the case of mixing in solution. Indeed, under these conditions, the initial contact of a chain with the MWNTs surface forms a CH–π interaction and successive CH groups gradually attach, leading to complete or partial adsorption of the polymer chain.

Due to this adsorption, the systems do not behave exactly as predicted by interfacial thermodynamics based on the surface properties of the neat components. This can be explained as follows: to transfer an MWNT from one polymer to the other, all the macromolecules of the first polymer should be desorbed from the surface to be replaced by macromolecules of the second polymer. However, the adsorption of macromolecules is partially irreversible due to the large number of contacts between the macromolecule and the surface, leading to very high desorption activation energy. This adsorption–desorption process has already been observed and explained by Zaikin et al. [45] for the redistribution of carbon black particles in immiscible polymer blends.

To conclude, we present a tentative explanation for the various observations in the systems presented here. When carbon nanotubes are first dispersed in PA, adsorption of PA macromolecules occurs on the nanotubes. If the predicted equilibrium position of the MWNTs is at the interface, the MWNTs will migrate torwards the interface but stay pinned on the PA side, as observed for the EA/PA6 blends (Fig. 19 – Method 1). On the other hand, if the predicted equilibrium position is the PA phase, the MWNTs will stay in the PA bulk phase, as observed in EA/PA12 blends (Fig. 20 – Method 1). When carbon nanotubes are first dispersed in EA, corresponding macromolecules adsorb, at least partially, on the nanotubes surface. If thermodynamics predict that the equilibrium position of the MWNTs is at the interface, the MWNTs will migrate torwards the interface and be jammed there, as observed for EA/PA6 blends (Fig. 19 – Method 2 and 3). On the other hand, if thermodynamics predict that the MWNTs equilibrium location is in PA, the MWNTs will migrate torwards the interface but EA adsorbed chains will prevent further migration due to the high energy required to fully desorb the EA chains. Assuming that the MWNTs are not fully covered with EA and/or that a part of the adsorbed chains can desorb, part of the MWNTs will migrate inside the PA nodules, as observed for EA/PA12 blends (Fig. 20 – Method 2 and 3).

4. Conclusions

We present here the confinement of a large fraction of unpurified and unfunctionalized carbon nanotubes at the interface of PA/EA polymer blends, taking advantage of irreversible polymer adsorption on MWNTs and their subsequent migration. Moreover, the final morphologies observed are stable even after a mixing time of 60 min. The migration of MWNTs has already been studied in the literature [14–26] but an interfacial confinement of unfunctionalized nanotubes has never been observed. Depending on the mixing strategy and on the PA used, the MWNTs are either at least partially located at the interface between the two polymers or in the PA phase. The localization of the carbon nanotubes is determined on the one hand by the interactions between the filler and the polymers and on the other hand by at least partially irreversible adsorption of one polymer at the surface of the nanotubes controlled by the mixing sequence. The irreversible adsorption is proved by TGA combined with separation techniques for the polymer/MWNT composites by filtration or centrifugation.

However, it is worth noting that in other systems [14–23] where adsorption could also occur, no jamming at the interface is observed. Further research should therefore be performed in that direction.

Acknowledgments

The authors thank Pr. P. Labbé from university Joseph Fourier (Grenoble, France) for lending under pressure filtration device. We also thank Nanocyl S.A. for providing the Nanocyl®-7000.

References

[1] Geuskens G, Gielens JL, Geshef D, Deltour R. European Polymer Journal 1987;23(12):993–5.
[2] Gubbels F, Blacher S, Vanlanthem E, Jerôme R, Deltour R, Brouers F, et al. Macromolecules 1995;28(5):1559–66.
[3] Cheah K, Forsyth M, Simon GP. Synthetic Metals 1999;102(1–3):1232–3.
[4] Sumita M, Sakata K, Hayakawa Y, Asai S, Miyasaka K, Tanemura M. Colloid and Polymer Science 1992;270(2):134–9.
[5] Levon K, Margolina A, Patashinsky AZ. Macromolecules 1993;26:4061–3.
[6] Iijima S. Nature 1991;354(6348):56–8.
[7] Ruan SL, Gao P, Yang XG, Yu TX. Polymer 2003;44(19):5643–54.
[8] Lau K, Hui D. Composites Part B Engineering 2002;33(4):263–77.
[9] Andrews R, Weisenberger MC. Current Opinion in Solid State and Materials Science 2004;8(1):31–7.
[10] Ren Y, Li F, Cheng H-M, Liao K. Carbon 2003;41(11):2177–9.
[11] Baughman RH, Zakhidov AA, de Heer WA. Science 2002;297(5582):787–92.

[12] Thorstenson ET, Ren Z, Chou T-W. Composites Science and Technology 2001;61(13):1899–912.
[13] Khare R, Bose S. Journal of Minerals and Materials Characterization and Engineering 2005;4(1):31–46.
[14] Pötschke P, Bhattacharyya AR, Janke A. Polymer 2003;44(26):8061–9.
[15] Pötschke P, Bhattacharyya AR, Janke A. Carbon 2004;42(5--6):965–9.
[16] Pötschke P, Kretzschmar B, Janke A. Composites Science and Technology 2007;67(5):855–60.
[17] Wu M, Shaw L. Journal of Applied Polymer Science 2006;99(2):477–88.
[18] Wu M, Shaw LL. International Journal of Hydrogen Energy 2005;30(4):373–80.
[19] Li Y, Simizu H. Macromolecules 2008;41(14):5339–44.
[20] Meincke O, Kaempfer D, Weickmann H, Friedrich C, Vathauer M, Warth H. Polymer 2004;45(3):739–48.
[21] Zou H, Wang K, Zhang Q, Fu Q. Polymer 2006;47(22):7821–6.
[22] Pötschke P, Pegel S, Claes M, Bonduel D. Macromolecular Rapid Comunications 2008;29:244–51.
[23] Göldel A, Kasaliwal G, Pötschke P. Macromolecular Rapid Communications 2009;30(6):423–9.
[24] Krasovitski B, Marmur A. The Journal of Adhesion 2005;81(7–8):869–80.
[25] Bose S, Bhattacharyya AR, Kodgire PV, Misra A. Polymer 2007;48(1):356–62.
[26] Bose S, Bhattacharyya AR, Kodgire PV, Misra A, Pötshke P. Journal of Applied Polymer Science 2007;106(5):3394–408.
[27] Wu D, Zhang Y, Zhang M, Yu W. Biomacromolecules 2009;10(2):417–24.
[28] Fenouillot F, Cassagnau P, Majesté JC. Polymer 2009;50(6):1333–50.
[29] Elias L, Fenouillot F, Majesté JC, Martin G, Cassagnau P. Journal of Polymer Science Part B Polymer Physics 2008;46(18):1976–83.
[30] Wu S. Polymer interface and adhesion, marcel. New York: Dekker Inc.; 1982.
[31] Son Y. Polymer 2001;42(3):1287–91.
[32] www.surface-tension.de/solid-surface-energy.htm.
[33] Bismarck A, Kumru ME, Springer J. Journal of Colloid and Interface Science 1999;217(2):377–87.
[34] Matsunaga T. Journal of Applied Polymer Science 1977;21(10):2847–54.
[35] Barber AH, Cohen SR, Wagner HR. Physical Review Letters 2004;92(18). 186103/1-4.
[36] Nuriel S, Liu L, Barber AH, Wagner HD. Chemical Physics Letters 2005;404(4–6):263–6.
[37] Dujardin E, Ebbesen TW, Krishnan A, Treacy MMJ. Advanced Materials 1998;10(17):1472–5.
[38] Neimark A. Journal of Adhesion Science and Technology 1999;13(10):1137–54.
[39] Kusner I, Srebnik S. Chemical Physics Letters 2006;430(1–3):84–8.
[40] Gurevitch I, Srebnik S. Chemical Physics Letters 2007;444(1–3):96–100.
[41] Meuer S, Braun L, Schilling T, Zentel R. Polymer 2009;50(1):154–60.
[42] Liy YT, Zhao W, Huang ZH, Gao YF, Xie XM, Wang XH, et al. Carbon 2006;44:1581–616.
[43] Xie YH, Soh AK. Materials Letters 2005;59(8–9):971–5.
[44] Baskaran D, Mays JM, Bratcher MS. Chemistry of Materials 2005;17(13):3389–97.
[45] Zaikin AE, Karimov RR, Arkhireev VP. Colloid Journal 2001;63(1):53–9.